THE ASTROPHYSICAL JOURNAL, 445:L47–L50, 1995 May 20

DETECTION OF MgCN IN IRC +10216: A NEW METAL-BEARING FREE RADICAL

L. M. ZIURYS[1] AND A. J. APPONI[2]
Department of Chemistry, Arizona State University, Tempe, AZ 85287-1604
M. GUÉLIN
Institut de Radio Astronomie Millimétrique, 300 Rue de la Piscine, F-38406, St. Martin d'Héres, France
AND
J. CERNICHARO
Centro Astronomico de Yebes, IGN E 19080, Guadalajara, Spain
Received 1994 December 23; accepted 1995 March 7

ABSTRACT

A new metal-containing molecule, MgCN, has been detected toward the late-type star IRC +10216, using the NRAO 12 m and IRAM 30 m telescopes. The $N = 11 \rightarrow 10$, $10 \rightarrow 9$, and $9 \rightarrow 8$ transitions of this species, which has a $^2\Sigma^+$ ground state, have been observed in the outer envelope of this object at 3 mm. For the $N = 11 \rightarrow 10$ transitions, the two spin-rotation components are clearly resolved and conclusively identify this new radical. These measurements imply a column density for MgCN of $N_{tot} \sim 10^{12}$ cm^{-2} in the outer shell, which corresponds to a fractional abundance of $f \sim 7 \times 10^{-10}$. This molecule, the metastable isomer of MgNC, is the third metal-bearing species thus far identified in the *outer* shell of IRC +10216, and its detection implies a ratio of MgNC/MgCN ~ 22/1. MgCN may be formed through a reaction scheme involving magnesium and HNC or CN, both prominent outer shell molecules, or through synthesis on grains.

Subject headings: ISM: abundances — ISM: molecules — line: identification — radio lines: stars — stars: individual (IRC +10216)

1. INTRODUCTION

Despite the success of ion-molecule chemistry, there are still some fundamental unanswered questions concerning interstellar molecules. One such problem concerns the molecular carriers of the cosmically abundant metallic elements, such as magnesium, iron, and sodium. One theory is that most of these elements, being refractory, are condensed out onto the surfaces of dust grains. Certainly, large depletions of these elements are found in diffuse gas (e.g., Sofia, Cardelli, & Savage 1994). On the other hand, some percentage of the metals may remain in the gas phase as atoms or molecules. Because of their low ionization potentials, the metallic elements are likely to exist in singly ionized form in the atomic state (e.g., Oppenheimer & Dalgarno 1974). It is thought that atomic metal ions are generally chemically inert. However, this conclusion has been based primarily on thermodynamic arguments that concern reactions of metal ions with very stable, closed-shell species (Ferguson & Fehsenfeld 1978). Recent laboratory experiments by Smith et al. (1983) have shown that metallic ions such as Na^+ can react via radiative association processes. Therefore, the formation of interstellar molecules containing the metallic elements may be possible.

Evidence that reactions with the metallic elements may indeed proceed has been the recent observations of metal-bearing compounds toward the circumstellar shell of the late-type carbon star IRC +10216. Up to the present, six metal-containing molecules have been detected toward this object. Four of these species are the closed-shell, stable metal halide compounds NaCl, KCl, AlCl, and AlF (Cernicharo & Guélin 1987; Ziurys, Apponi, & Phillips 1994), while the remaining molecules, MgNC (Guélin et al. 1986; Kawaguchi et al. 1993) and NaCN (Turner, Steimle, & Meerts 1994), contain the cyanide moiety. The metal halides appear to come from the hot, dense inner part of the circumstellar envelope, where chemical thermodynamic equilibrium prevails. MgNC (and probably NaCN), however, originate in the outer part of the expanding shell (Guélin, Lucas, & Cernicharo 1993), where temperatures and densities are sufficiently low such that the chemistry is kinetically controlled and photochemical and ion-molecule processes occur (e.g., Cherchneff, Glassgold, & Mamom 1993). The outer shell chemical pathways produce reactive free radicals, including presumably MgNC, which are too unstable to exist in the inner envelope. Thus, metal chemistry in IRC +10216 appears to take place throughout the circumstellar shell and must involve a variety of synthetic processes. Clearly, metals may not be as inert as models tend to suggest, nor can they all be contained in dust grains.

As part of our ongoing program of examining the carriers of the metallic elements, we have conducted a search for a new possible metal-containing molecule, MgCN. MgCN is the metastable isomer of MgNC. We have detected this species toward the outer envelope of IRC +10216, observing its $N = 11 \rightarrow 10$, $10 \rightarrow 9$, and $9 \rightarrow 8$ rotational transitions at 3 mm using both the NRAO[3] 12 m and IRAM 30 m telescopes. These observations were done based on rest frequencies measured in our laboratory (Anderson, Steimle, & Ziurys 1994). In this Letter we report our results.

2. OBSERVATIONS

The measurements employing the NRAO 12 m telescope, located at Kitt Peak, Arizona, were carried out 1993 May/October and 1994 May. The receiver used was a dual-channel, cooled SIS mixer operated in a single-sideband mode with over 20 dB image rejection. The temperature scale was determined

[1] Presidential Faculty Fellow.
[2] NASA Space Grant Fellow.
[3] NRAO is operated by the Associated Universities, Inc., under contract with the National Science Foundation.

TABLE 1

OBSERVATIONS OF MgCN TOWARD IRC +10216[a]

		NRAO 12 m[c]						IRAM 30 m[d]					
TRANSITION	FREQUENCY[b] (MHz)	θ_b	η_c	T_R^* (mK)	V_{LSR} (km s^{-1})	$\Delta V_{1/2}$ (km s^{-1})	$\int T_R^* dv$ (K km s^{-1})	θ_b	η_B	T_A^* (mK)	V_{LSR} (km s^{-1})	$\Delta V_{1/2}$ (km s^{-1})	$\int T_A^* dv$ (K km s^{-1})
$N = 11 \rightarrow 10$:													
$J = 21/2 \rightarrow 19/2$...	112063.4	57″	0.84	4 ± 2	-26.0 ± 2.1	30.3 ± 4.2	0.12 ± 0.01	22″	0.60	6 ± 2	-26.4 ± 1.3	29.4 ± 2.7	0.11 ± 0.02
$J = 23/2 \rightarrow 21/2$...	112078.4	...	...	4 ± 2	-27.4 ± 2.1	~ 30	~ 0.12	...	...	6 ± 2	-27.4 ± 1.3	26.7 ± 2.7	0.10 ± 0.02
$N = 10 \rightarrow 9$:													
$J = 19/2 \rightarrow 17/2$...	101877.6	62″	0.86	...[e]	...	...	...	23″	0.60	...[e]	...	...	...
$J = 21/2 \rightarrow 19/2$...	101892.6	...	...	2 ± 0.5	-26.0 ± 5.9	35.3 ± 5.9	0.07 ± 0.01	...	...	6 ± 2	-27.6 ± 1.8	29.4 ± 2.9	0.09 ± 0.02
$N = 9 \rightarrow 8$:													
$J = 17/2 \rightarrow 15/2$...	91690.9	...	...	...	...	...	...	27″	0.60	~ 8[f]	~ -26[f]	~ 30[f]	...
$J = 19/2 \rightarrow 17/2$...	91705.9	...	...	...	...	...	...	...	...	~ 10[f]	~ -26[f]	~ 30[f]	...

[a] Errors are 3 σ; observations taken toward $\alpha = 9^h45^m14^s.8$, $\delta = 13°30'40''$ (1950.0).
[b] From Anderson, Steimle, & Ziurys 1994.
[c] Measured with 0.781 MHz resolution for 112 GHz data; 2 MHz resolution for 101 GHz observations.
[d] Measured with 1 MHz resolution.
[e] Obscured by C_6H.
[f] Blended with c-C_3H.

by the chopper wheel method, corrected for forward spillover losses, and is given in terms of T_R^*. The back ends employed were two 256 channel filter banks with 1 and 2 MHz resolution, respectively, used in parallel mode (2×128 channels) with both receiver channels. A 2×768 channel hybrid spectrometer with 781 kHz resolution was also used in a parallel mode.

The data obtained with the IRAM 30 m telescope at Pico Veleta, Spain, were taken 1994 June and November. The receiver used was a single-channel, cooled SIS mixer, with image rejection between the 10 dB (1994 June) and 30 dB (1994 November) levels. The temperature scale is in terms of T_A^*. The back end employed was a 256 channel filter bank with 1 MHz resolution.

All data were taken in a beam switching mode toward the position $\alpha = 9^h45^m14^s.8$, $\delta = 13°30'40''$ (1950.0). The intermediate frequency for both telescopes was 1.5 GHz, except the 12 m data was taken in the USB and the 30 m measurements in the LSB. Observing frequencies, beam sizes, and beam efficiencies η_c and η_B are given in Table 1. Local oscillator shifts were performed for all measurements to minimize possible image contamination. (The IRAM spectral survey of IRC +10216 was also checked to insure that no line stronger than 50 mK was present in the image sideband near the MgCN frequencies.)

3. RESULTS

MgCN has a $^2\Sigma^+$ ground electronic state, and thus every transition is split into doublets owing to spin-rotation interactions. The average spin-rotation splitting for MgCN is 15.0 MHz (Anderson et al. 1994) and should be at least partially resolved at 3 mm in IRC +10216.

Figure 1 presents the data obtained for MgCN at 2 MHz resolution using the 12 m telescope, which only includes the $N = 11 \rightarrow 10$ and $10 \rightarrow 9$ transitions near 112 and 101 GHz. As the figure shows, the doublet structure is apparent in the 112 GHz spectrum, and the line profiles are roughly flat topped. The MgCN emission is thus not resolved in the $\sim 60''$ beam. In the 101 GHz data, however, the lower frequency spin component of MgCN is contaminated by the $J = 36.5 \rightarrow 35.5$ transition of C_6H. The MgCN feature is still visible as a "shoulder" on the C_6H profile. The higher frequency component of the doublet is unobscured.

Figure 2 shows the 12 m spectrum of the $N = 11 \rightarrow 10$ transition of MgCN observed with the hybrid correlator (0.781 MHz per channel). The higher resolution used here clearly separates out the two spin doublets of MgCN.

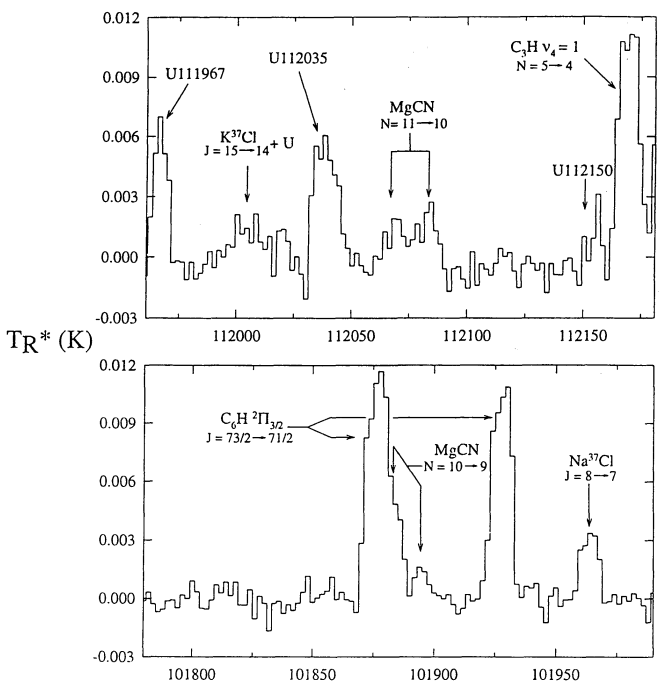

FIG. 1.—Spectrum of the $N = 11 \rightarrow 10$ and $10 \rightarrow 9$ transitions of MgCN, observed with the NRAO 12 m telescope at 112 and 102 GHz, respectively, towards IRC +10216 using 2 MHz resolution. The assumed LSR velocity is -26.4 km s^{-1}. Both spin-rotation components are clearly visible in the $N = 11 \rightarrow 10$ spectrum. In the $N = 10 \rightarrow 9$ data, one component is uncontaminated, but the other appears as a weak shoulder on a C_6H line.

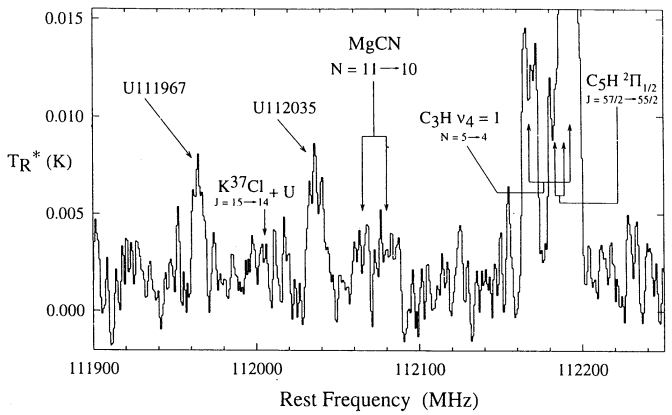

FIG. 2.—Spectrum of the $N = 11 \rightarrow 10$ transition of MgCN observed with the 12 m telescope toward IRC +10216, but using 0.781 MHz resolution. The doublet structure of this transition is apparent in these data.

In Figure 3, the spectra obtained with the IRAM 30 m are presented, which include $N = 9 \rightarrow 8$ data as well as $N = 11 \rightarrow 10$ and $10 \rightarrow 9$ measurements. For these observations, the beam size was $<30''$ (see Table 1), and the spectral resolution was 1 MHz. In the $N = 11 \rightarrow 10$ data, the two MgCN spin-rotation components are clearly resolved and appear to show the cusped profile indicating that the source is resolved in the $\sim 22''$ beam of the 30 m. Two weak features at the right of the MgCN spectrum suggest a higher noise level that is actually present; these features are visible in both the June and November data and are most likely *U* lines.

The $N = 10 \rightarrow 9$ spectrum in Figure 3 from IRAM resembles the 12 m data, but the higher resolution (1 vs. 2 MHz) better separates the MgCN "shoulder" on the C_6H profile.

In the $9 \rightarrow 8$ data, both components of MgCN are blended with two transitions of cyclic C_3H at 91692.7 and 91699.5 MHz. The two C_3H lines are quite close in frequency, however, and cannot account for the broad, 82 km s^{-1} wide feature that has been observed. The total spread of the C_3H lines should be only 53 km s^{-1}, based on the well-known IRC +10216 line width of 29 km s^{-1}. The additional emission can readily be attributed to the spin components of MgCN, which occur to either side of C_3H, as the figure shows. In addition, the $J = 2 \rightarrow 1$ transition of $^{13}C^{33}S$ is at 91685.3 MHz, i.e., on the left side of the $J = 17/2 \rightarrow 15/2$ component of MgCN. The contribution of $^{13}C^{33}S$, however, should be <1 mK, considering the observed $^{12}C^{33}S$ $J = 2 \rightarrow 1$ line temperature of 30 mK and the $^{12}C^{34}S/^{13}C^{34}S$ intensity ratio of 40–50, measured by Kahane et al. (1988).

Table 1 lists the line parameters determined for MgCN from both the 12 m and IRAM measurements. As the table illustrates, the 12 m intensities for MgCN are $T_R^* \sim 2$–4 mK, while those from the 30 m are $T_A^* \sim 6$–10 mK ($T_R^* = T_A^*/0.9$). The difference in intensities is primarily because of the varying beam sizes used. Plateau de Bure interferometer maps (Guélin et al. 1993) suggest that MgNC has a shell-like distribution with a radius of $r \sim 15''$. If one assumes a similar distribution for MgCN and corrects for beam dilution, then the antenna temperatures from the two telescopes agree to within 30%.

Table 1 also lists the measured line widths, LSR velocities, and integrated intensities for MgCN. The fitted velocities are $V_{LSR} = -26$–28 km s^{-1} and, within the errors, are equal to the systemic velocity of the shell (i.e., -26.4 km s^{-1}, according to the C_3H lines in Fig. 3). Furthermore, the line widths have an average of ~ 29 km s^{-1}, as is typically found for outer envelope molecules (e.g., Kahane et al. 1988).

4. DISCUSSION

4.1. *Column Densities and Abundances*

MgCN appears to be resolved in the IRAM beam and thus probably exists in the outer envelope, where its isomer MgNC is present. A multitransition study of MgNC by Guélin et al. (1994) suggests $T_{rot} \sim 20$ K and $N_{tot} = 5 \times 10^{13}$ cm^{-2} for this molecule. Recent calculations for the UMP2F-6311 + 63 *df* level by P. Valiron (private communication) indicate that the dipole moments of MgCN and MgNC are almost identical (5.3 and 5.5 D, respectively, with an error of ± 0.2 D). Therefore, the column density of MgCN can be estimated from the line intensity ratio of MgNC/MgCN. For the unblended 3 mm line components, this ratio is 22 ± 3 (see Guélin et al. 1994). This value implies that the column density of MgCN is $N_{tot} \sim 2 \times 10^{12}$ cm^{-2}. An LTE calculation (see Ziurys, Hollis, & Snyder 1994) gives an almost identical value for the column density, using $T_{rot} = 20$ K and the $N = 11 \rightarrow 10$ transition.

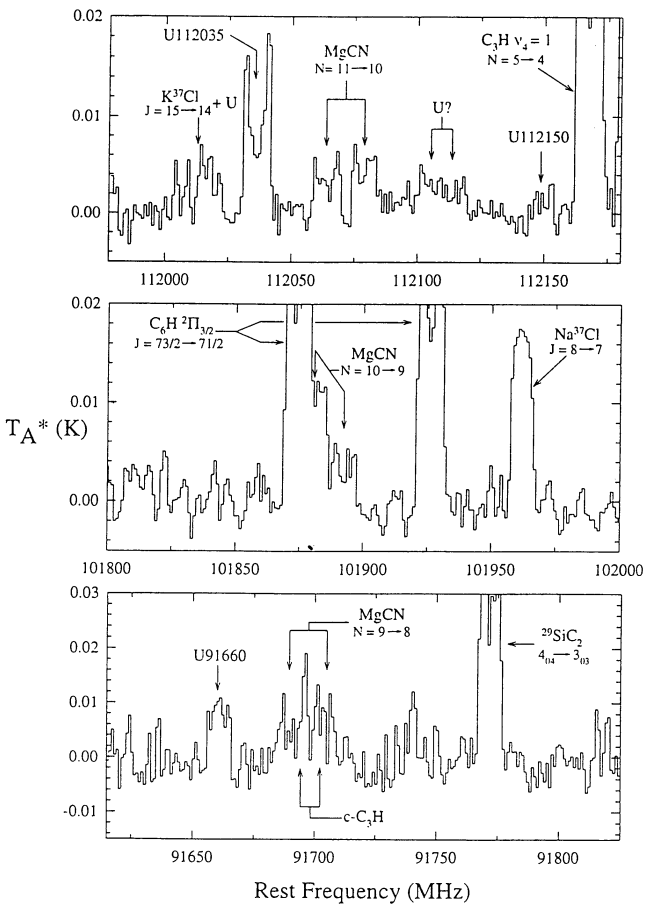

FIG. 3.—Spectrum of the $N = 11 \rightarrow 10$, $10 \rightarrow 9$, and $9 \rightarrow 8$ transitions of MgCN obtained with the IRAM 30 m telescope toward IRC +10216 at 112, 102, and 92 GHz, using 1 MHz resolution. Assumed LSR velocity is -26.4 km s^{-1}. The $N = 11 \rightarrow 10$ spin-doublets are clearly resolved in these data. Again, one doublet of the $N = 10 \rightarrow 9$ transition is partially obscured by C_6H. For the $N = 9 \rightarrow 8$ lines, the center of the two doublets is contaminated by c-C_3H, but MgCN emission is distinctly present.

To obtain a fractional abundance for MgCN, a molecular hydrogen column density of $N(H_2) \sim 3.0 \times 10^{21}$ cm^{-2} has been adopted, which assumes that this radical has a flat distribution between $r = 10''$ and $r = 20''$, or between $r = 3 \times 10^{16}$ and 6×10^{16} cm from the star, like MgNC. The H_2 column density is derived for a mass loss of $4 \times 10^{-5}\ M_\odot$ yr^{-1} and a distance of 200 pc (Truong-Bach, Morris, & Nguyen-Q-Rieu 1993). The fractional abundances of MgCN then is $\sim 7 \times 10^{-10}$. This value accounts for $\sim 10^{-5}$ of the cosmic abundance of magnesium, and therefore only a small amount of this element is contained in MgCN.

4.2. *Relationship of* MgCN *and* MgNC

Theoretical calculations predict that MgCN lies ~ 700 K higher in energy than MgNC, with a barrier to conversion of ~ 300 K (Ishii et al. 1993). Therefore, the cyanide is metastable and is likely to be less abundant than its isocyanide counterpart, depending on the relative formation mechanisms. Our ratio of MgNC/MgCN $\sim 22/1$ in the outer envelope of IRC +10216 implies a mechanism that is reasonably favorable for both isomers.

Kawaguchi et al. (1993) suggest that MgNC in IRC +10216 is formed via the radiative association of $Mg^+ + HCN \rightarrow MgNCH^+ + h\nu$, followed by electron dissociative recombination to produce MgNC + H. The radiative association process is used because most ion-molecule reactions of Mg^+ are thought to be endothermic. In analogy, MgCN could be synthesized by the following scheme:

$$Mg^+ + HNC \rightarrow MgCNH^+ + h\nu\,, \quad (1)$$

$$MgCNH^+ + e^- \rightarrow MgCN + H\,. \quad (2)$$

This pathway is far more likely than direct conversion from MgNC because of the large barrier for isomerization. Therefore, if the rates for the radiative association reactions are similar, then the MgNC/MgCN ratio may reflect that of HCN/HNC in the outer envelope.

Unlike the magnesium isomers, the distributions of HCN and HNC in IRC +10216 are not similar. HCN arises primarily from chemistry occurring deep in the envelope of IRC +10216, while HNC is located almost entirely in the outer shell (e.g., Bieging & Rieu 1988). Some measurements, however, have been made of $H^{13}CN$ in the outer shell, and it is found that the abundance of this species is at least three times that of HNC (Bieging & Rieu 1988; Cernicharo et al. 1987; Dayal & Bieging 1995). Again, using the $^{12}C/^{13}C$ ratio derived by Kahane et al. (1988), the implied HCN/HNC ratio is > 120, far greater than the measured MgNC/MgCN ratio.

Another possibility is that both MgCN and MgNC are formed through the radiative association reaction of neutral Mg and the CN radical. CN is very abundant in the outer shell, being produced from the photodestruction of HCN (e.g., Bieging, Chapman, & Welch 1984). The isocyanide might be the favored product of such a process because of the polarity of the cyanide moiety, $C^{\delta+}N^{\delta-}$, and the fact that magnesium has unfilled *d* orbitals.

4.3. *Implications for Metal Chemistry*

Detection of MgCN brings the number of metal-bearing molecules found in the outer shell of IRC +10216 to three, along with MgNC and probably NaCN. All three compounds are metal cyanide/isocyanide species. While the two magnesium compounds are radicals, NaCN is a closed-shell molecule that is T-shaped in geometry. The Na atom in this species "orbits" the CN group, and there is consequently no preferred cyanide or isocyanide form. (NaCN could also be described structurally as NaNC.) One might expect that NaCN would have a high concentration in the inner circumstellar envelope because of its closed-shell, stable structure. Its presence in the outer envelope is only supported by its cusped line shape, observed with the 30 m telescope. The "cusps" are not as prominent as those of MgNC, however, and the species may have some inner envelope distribution.

If identical assumptions are used for NaCN as for the magnesium compounds, then the column density derived for this species is $N_{tot}(NaCN) \sim 1.5 \times 10^{13}$ cm^{-3}, using the data of Turner et al. (1994). Such a value implies a fractional abundance for this species of $f \sim 5 \times 10^{-9}$, and consequently 3[NaCN] $\cong$ [MgNC] + [MgCN]. Therefore, the concentrations of cyanide/isocyanide metal-bearing compounds in the outer envelope of IRC +10216 do not reflect the cosmic abundances of the respective metals, which have the ratio Mg/Na $\sim$ 17. Also, only a small fraction of the metallic elements thus far have been found to be contained in molecular form, with about 10^{-4} for Mg and approximately 10^{-3} for Na.

Another option for the synthesis of the metal-CN compounds is desorption from grain mantles, as discussed by Guélin et al. (1993). These authors argue that the short timescales for outer shell chemistry imply a fast production scheme, such as loss of molecules from a grain surface. Grain heating by interstellar UV photons penetrating inside the envelope (the same photons that dissociate HCN) and/or mild shocks could release the adsorbed radicals into the gas phase. Because surface processes are not well understood, it is difficult, however, to elaborate further on this possibility. Clearly, more observational and laboratory data are required to understand metal chemistry in IRC +10216.

This research is supported by NSF grant AST-92-53682 and NASA grant NAGW 2989. L. M. Z. thanks NRAO for travel funds to IRAM. We also thank Pierre Valiron for communicating results prior to publication.

REFERENCES

Anderson, M. A., Steimle, T. C., & Ziurys, L. M. 1994, ApJ, 429, L41
Bieging, J. H., Chapman, B., & Welch, W. J. 1984, ApJ, 285, 656
Bieging, J. H., & Rieu, N.-Q. 1988, ApJ, 329, L107
Cernicharo, J., & Guélin, M. 1987, A&A, 183, L10
Cernicharo, J., Guélin, M., Menten, K. M., & Walmsley, C. M. 1987, A&A, 181, L1
Cherchneff, I., Glassgold, A. E., & Mamom, G. 1993, ApJ, 410, 188
Dayal, A., & Bieging, J. H. 1995, ApJ, 439, 996
Ferguson, E. E., & Fehsenfeld, F. C. 1978, J. Geophys. Res., 73, 6125
Guélin, M., Cernicharo, J., Kahane, C., & Gomez-Gonzales, J. 1986, A&A, 157, L17
Guélin, M., Forestini, M., Valiron, P., Ziurys, L. M., Anderson, M. A., Cernicharo, J., & Kahane, C. 1994, A&A, in press
Guélin, M., Lucas, R., & Cernicharo, J. 1993, A&A, 280, L19
Kahane, C., Gomez-Gonzales, J., Cernicharo, J., & Guélin, M. 1988, A&A, 190, 167
Kawaguchi, K., Kagi, E., Hirano, T., Takano, S., & Saito, S. 1993, ApJ, 406, L39
Ishii, K., Hirano, T., Nagashima, U., Weis, B., & Yamashita, K. 1993, ApJ, 410, L43
Oppenheimer, M., & Dalgarno, A. 1974, ApJ, 192, 29
Smith, D., Adams, N. G., Alge, E., & Herbst, E. 1983, ApJ, 272, 365
Sofia, U. J., Cardelli, J. A., & Savage, B. D. 1994, ApJ, 430, 650
Truong-Bach, Morris, D., & Nguyen-Q-Rieu. 1991, A&A, 249, 435
Turner, B. E., Steimle, T. C., & Meerts, L. 1994, ApJ, 426, L97
Ziurys, L. M., Apponi, A. J., & Phillips, T. G. 1994, ApJ, 433, 729
Ziurys, L. M., Hollis, J. M., & Snyder, L. E. 1994, ApJ, 430, 706